THE JOURNAL OF PHYSICAL CHEMISTRY B

Article

pubs.acs.org/JPCB

Effects of Embedded Carbon Nanotube on Properties of Biomembrane

Xiaoyi Li,*[,†,‡] Yanchao Shi,[†,‡] Bing Miao,[‡] and Yuliang Zhao*[,†]

[†]Key Laboratory for Biomedical Effects of Nanomaterials & Nanosafety, National Center for Nanosciences and Technology of China, Beijing 100191, and Institute of High Energy Physics, Chinese Academy of Sciences, Beijing 100049, P. R. China

[‡]College of Materials Science and Opto-electronics Technology, Graduate University of Chinese Academy of Sciences, Beijing 100049, P. R. China

ABSTRACT: We investigated the interaction between embedded nanotube and biomembrane using molecular dynamics (MD) simulations. The effects of embedded nanotube on biomembrane were characterized by investigating the influence on the conformational fluctuation of individual lipid molecules, the organization of membrane molecules, the diffusion behavior of lipid molecules, and the diffusion behavior of penetrants inside biomembrane. The steric interaction with the nanotube leads to an entropy reduction of interfacial membrane molecules, while the long-range electrostatic interaction with the N-DWCNT enhances the conformational fluctuation of lipid molecules. The curvature of embedded nanotube could also influence the flexibility of lipid molecules. When the interaction between nanotube and the membrane molecules is weak, the packing density of the membrane is almost unaffected. On the contrary, when the attraction between nanotube and the membrane molecules significantly increases, the attraction among the membrane molecules decreases effectively, which leads to a relaxation of the organization of membrane. With the increase of the strength of electrostatic interaction between nanotube and small polar molecules, interaction-modified friction increases, which leads to the decrease of the diffusion constant of penetrants inside the biomembrane.

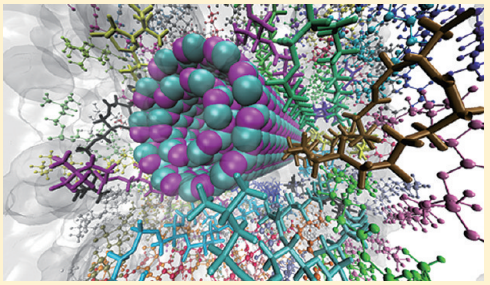

INTRODUCTION

Nanotechnology has been broadly applied in materials science, sensing, bioimaging, biomedicine, and biology, which made us inevitably exposed to nanomaterial.[1−5] Recent studies on eukaryotic and prokaryotic cells have shown that nanomaterial used for biomedical applications may in fact induce cytotoxic effects.[6−10] In addition, functionalized nanoparticles enable their use in broader applications such as environment[11] and industry.[12] However, the engineered nanoparticles can also interact with biological molecules and have potential to damage cells in vivo.[13] Thus, investigation of the effects of nanomaterial on biological systems is paramount.

Many studies have been conducted on the interactions between cell membranes and several types of nanoparticles including fullerenes, carbon nanotubes (CNTs), and gold nanoparticles.[14−18] Bedrov et al.[19,20] and Wong-Ekkabut et al.[21] found that translocation of fullerene and its cluster into a biomembrane is energetically favorable and that these particles tend to sit off the bilayer center,[22] while modified C60 was shown to be prohibited from translocating across the membrane layer, suggesting a method to control transport across a bilayer.[23,24] Charged nanoparticles could result in membrane breakage leading to cytotoxic effects.[25] Functionalized nanoparticles have been used to select only particular cellular membranes so that only specific cells are labeled.[26] Graphene is found to be able to translocate into a biomembrane.[27]

Coarse grained molecular dynamics and theoretical studies have shown that CNTs with sufficiently small radii can directly pierce through a cell membrane, while larger tubes tend to enter the cell via a wrapping mechanism.[28] However, lipids in the bilayer can block the nanotube upon piercing the membrane.[29] Furthermore, the cylindrical micelle of lipids may be utilized to solubilize carbon nanotubes.[30]

Recent publications of charged nanoparticles on electroneutral phospholipids bilayers revealed that electrostatic attraction improves the adhesion of a charged nanoparticle to the membrane, where the increase of electrostatic energy results in almost full wrapping of the charged nanoparticle by the membrane.[31] Li et al.[32] have reported that the surface hydrophobicity can result in different response mechanisms for nanoparticle−biomembrane interactions.

Detailed understanding of the effects of inserted nanoparticles on biomembrane is crucial for the reduction of possible cytotoxic effects.[33] Studies of CNTs inserted in lipid bilayers showed that the CNTs have an effect on the local structure and dynamics of the biomembrane.[34−37] In the simulations of Nielsen et al.,[34] the length of the nanotube was varied to assess the effects of hydrophobic mismatch at the nanotube-lipid boundary. Liu and Hopfinger[35] studied the

Received: February 24, 2012
Revised: April 18, 2012
Published: April 19, 2012

dx.doi.org/10.1021/jp301864z | J. Phys. Chem. B 2012, 116, 5391−5397

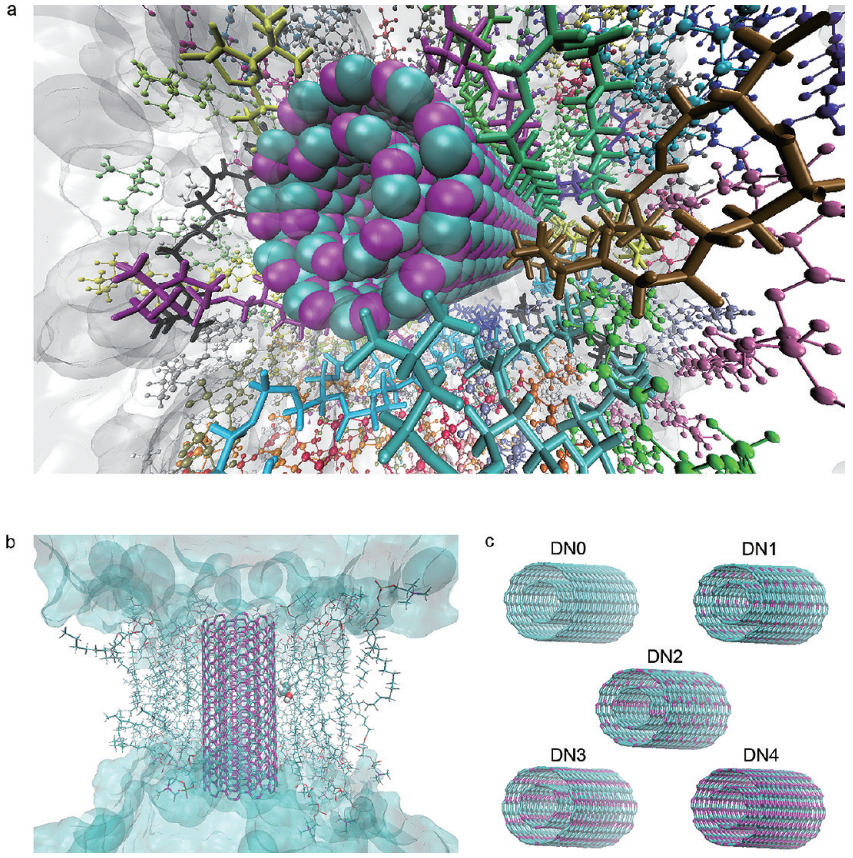

Figure 1. Overview of the simulation system: (a) DMPC and N-DWCNT assembly with water. Interfacial lipid molecules are drawn in licorice style; noninterfacial lipid molecules are drawn in CPK style. (b) DMPC and N-DWCNT assembly with ethanol inside DMPC and water. (c) N-DWCNT model with different proportion of N atoms. In a–c, all nitrogen atoms in CNTs are colored in magenta; carbon atoms are colored in cyan.

possible sources of nanotoxicity from carbon nanotubes inserted into biomembrane using structure–activity relationship analysis. We have reported that the diffusion of lipids is hindered by the inserted CNT.[36] In addition, experimental data also indicated that different size, shape, and modification of nanotubes exhibit different cytotoxicity.[38,39] However, how the inserted nanotube influences the structure and function of biomembrane, and what the dominant force is that determines the disturbance on biomembrane remain ambiguous.

In this study, we designed the model of nanotube–biomembrane assembly by embedding the single-walled nanotube (SWCNT), double-walled nanotube (DWCNT), or the nitrogen-doped double-walled nanotube (N-DWCNT) into dimiristoylphosphatidylcholine (DMPC) membranes. We investigated the interaction between embedded nanotube and biomembrane using molecular dynamics (MD) simulations. We characterized the effects of embedded nanotube on biomembrane by investigating the influence on the conformational fluctuation of individual lipid molecules, the organization of membrane molecules, the diffusion behavior of lipid molecules, and the diffusion behavior of penetrants inside biomembrane.

In addition, on the basis of the Einstein relationship, which links the characteristics of the response behavior of a system, friction constant, to the characteristics of the fluctuation behavior of a system, diffusion constant, we proposed the effective friction constant to explore the diffusion behavior of two small polar molecules inside biomembrane.

MODEL DESIGN

As shown in Figure 1, a nitrogen-doped double-walled carbon nanotube with armchair type (11,11) as the outer tube and (6,6) as the inner tube was designed. The diameter of the inner tube is around 8 Å, and the space between the tubes is around 3.4 Å. The uncapped N-DWCNT with a length of 33 Å was embedded into the DMPC bilayer membrane. The doping concentrations of nitrogen in N-DWCNTs were designed to be 0%, 11%, 18%, 25%, and 50% in models DN0, DN1, DN2, DN3, and DN4, respectively. In addition, a nitrogen-doped single-walled carbon nanotube with 50% of nitrogen atoms was embedded into DMPC, denoted as model SN4, and a net DMPC membrane model was built for comparison. Two equivalent charges (+0.25e) were assigned to a pair of next-nearest-neighboring carbon atoms roughly at the middle of the inner tube to mimic the asparagine-proline-alanine (NPA) region of aquaporin (AQP) proteins.[40,41] Sodium and chloride ions were added into the solvent at the concentration of 0.15 M to keep the physiological condition.

To investigate the diffusion behavior of small polar molecules in the DMPC and N-DWCNT assembly, urea and ethanol were placed originally near the tail of the lipid molecule, as shown in Figure 1b.

SIMULATION DETAILS

Molecular dynamics simulations were performed by program NAMD (Version 2.8)[42] in NPT ensembles with periodic boundary conditions. The CHARMM27 force field and the CHARMM General Force Field were used.[43,44] The parameters

dx.doi.org/10.1021/jp301864z | J. Phys. Chem. B 2012, 116, 5391–5397

for the carbon atoms were those of type CA, corresponding to the parameters of benzene in CHARMM27 force field. All the parameters of nitrogen atoms adopt the most common ones, used in peptide nitrogen (named NH1 in CHARMM27), amide nitrogen (named NH2), and nitrogen in pyrrole ring (named NY), except the partial charge. We used the average QM HF-6-31G** EPS fitting charges with a 50% N-doped CNT as a template for the partial charges of all nitrogen atoms, which was averaged to approximately −0.39e. Electrostatic interactions were calculated by particle mesh Ewald method (PME).[45] The DMPC membrane was downloaded from the Web site of Klauda's group.[46] The membrane and water assembly was performed for a 30 ns equilibration at 1 atm and 310 K without any restraint. We ran a 30 ns MD simulation after 2 ns equilibration and collected data every 1 ps. The details of creating the cylinder hole in the DMPC membrane and embedding the nanotubes into the hole were described in our previous work.[36]

The parameters of urea and ethanol adopt that in the CHARMM General Force Field v. 2b7 for small molecule drug design. All systems were run for 200 ps for equilibration, with the penetrants restrained. After that, we ran it for 4 ns without any restraint at 1 atm and 310 K. The data of the last 3 ns was collected for statistics.

RESULTS AND DISCUSSION

Effect of Embedded Nanotube on the Conformational Fluctuation of Individual DMPC Molecule. A biomembrane is a separating membrane that acts as a selective barrier around a cell. Biomembrane could be described as a highly viscous fluid matrix of a bilayer of phospholipids having globular proteins associated with them.[47] Thus, the conformations of individual DMPC molecules are fluctuating with time.

We investigated the conformational fluctuation of each individual DMPC molecule by the root-mean-square deviation (rmsd). Rmsd is a numerical measure of the difference between two structures and reveals the average conformational evolution over time. It is defined as

$$\mathrm{rmsd} = \sqrt{\frac{\sum_{i=1}^{N_{\mathrm{atoms}}} (r_i(t_1) - r_i(t_2))^2}{N_{\mathrm{atoms}}}} \quad (1)$$

where N_{atoms} is the number of atoms whose positions are compared, and $r_i(t)$ is the position of atom i at time t.

Rmsds were calculated by the rmsd trajectory tool in VMD[48] with a frame span of 1 ps and the average structure as the reference. Table 1 summarized the average rmsds for all models.

Distinguishing interfacial DMPC from noninterfacial DMPC may be of significance for studying the interaction between the nanotube and the biomembrane. We defined the interfacial DMPC as the lipids that are less than 5 Å away from the outer nanotube wall. There are 72 lipid molecules in each model; 20−24 of them are interfacial lipid molecules in models with embedded DWCNT, and 14−18 of them are interfacial molecules in models with embedded SWCNT.

Table 1. Rmsds Averaged on Individual DMPC Molecules

	DN0	DN1	DN2	DN3	DN4	SN4	net DMPC
rmsd of interfacial DMPC (Å)	1.83	2.03	2.21	2.20	2.06	1.87	2.24
rmsd of total DMPC (Å)	1.96	2.43	2.66	2.53	2.38	1.94	2.24

From Table 1, we could see that the interfacial lipid molecules have appreciably smaller average rmsds compared with the corresponding rmsds averaged on the total DMPC molecules in all the models. In addition, rmsds averaged on the interfacial lipid molecules in all models with embedded CNTs are smaller than that averaged on net DMPC molecules. This is understandable considering that the embedded CNT reduces the entropy of interfacial lipid molecules due to its rigid and unaccommodating structure, and leads to fewer conformational states available to DMPC molecules adjacent to the tube.

The rmsd averaged on total lipid molecules in model DN0 is smaller than that in net DMPC, which indicates again that the lipid molecule loses the displacement and becomes more rigid with embedded DWCNT.

However, when the embedded DWCNT is doped with nitrogen atoms, the situation is totally different. The rmsds averaged on all lipid molecules with N-DWCNT embedded are bigger than that averaged on net DMPC molecules, which reveals that the structure of lipid molecules becomes more flexible when it is embedded with N-DWCNT.

The reason lies in the fact that the most significant difference between these two cases is that the partial charges are distributed on the N-DWCNT, while there is not any charge on DWCNT. Our observation indicates that the long-range electrostatic interaction between N-DWCNT and DMPC enhances the conformational fluctuation of lipid molecules and thus increases their rmsds.

The results above reveal that the steric interaction with the nanotube leads to an entropy reduction of interfacial lipids and thus reduces the rmsds of the interfacial lipids, while the long-range electrostatic interaction with the N-DWCNT excites the conformational fluctuation of lipid molecules. The steric interaction and the long-range electrostatic interaction play their effects oppositely, which results in the reduction of rmsds for interfacial lipids and the increase of rmsds averaged on all lipid molecules with embedded N-DWCNT.

We can also see from Table 1 that the rmsd of lipids with embedded N-SWCNT is smaller than that with embedded N-DWCNT, indicating that the curvature of embedded nanotube could also influence the flexibility of lipid molecules.

Effect of Embedded Nanotube on the Organization of Membrane. In addition to the conformational fluctuation of individual lipid molecules, we are also interested in the influence of embedded nanotubes on the organization of membrane.

The packing density of the membrane, calculated from the area per molecule (APM), is used to characterize the organization of bilayer membrane. In fact, APM is one of the fundamental features used to characterize the total structure of a lipid membrane and is also a useful measure to monitor the equilibration process in the molecular dynamics study of a membrane assembly.

To define the area per lipid molecule (APM) in the bilayer plane, we made a two-dimensional Voronoi tessellation analysis (Figure 2) for the centers of mass of lipid molecules projected onto the bilayer plane under the periodic boundary condition.[49] A single-molecular area A_i was, then, defined by the area of Voronoi polygon i. The number of sides of a Voronoi polygon i gives a definition of the number of nearest neighbor molecules

dx.doi.org/10.1021/jp301864z | J. Phys. Chem. B 2012, 116, 5391−5397

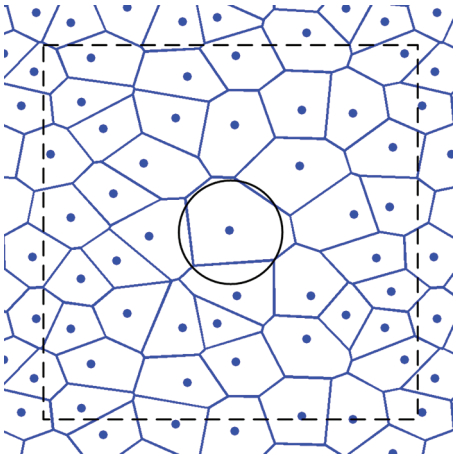

Figure 2. Voronoi tessellation. Nanotube is located at the region of the black circle. The black dotted line is the boundary of the simulation biomembrane.

of the lipid. Using this, the molecular area of the total system A^N can be written by

$$A^N = \sum_i^N Ai/2 \tag{2}$$

where N is the total number of lipid molecules in the system, which includes the upper and lower layers.

The APMs of our models are shown in Table 2. The APMs of model DN0, DN3, and DN4 are very close to that of net DMPC, which means that the packing density of DMPC membrane in these three models are almost not disturbed by the embedded N-DWCNT. At the same time, the APM of model DN1 and DN2 increases apparently compared to that of net DMPC, indicating that the organization of membrane is relaxed.

Table 2. Area Per Molecule (APM) of DMPC Lipid

	DN0	DN1	DN2	DN3	DN4	net DMPC
APM (Å^2)	48.35	78.94	64.06	52.54	55.30	51.94

This phenomenon can be understood from the viewpoint of the effective interaction. Specifically, APM is determined by the effective interaction between the membrane molecules. In the present model, the effective interaction between the membrane molecules comes from a competition between the membrane molecule−membrane molecule attraction and the nanotube−membrane molecule attraction. When the nanotube−membrane molecule attraction is weak, corresponding to the cases of DN0, DN3, and DN4, the effective membrane molecule−membrane molecule interaction is not modified much by the presence of nanotube, and this leads to the observation that the APM in this situation is close to that for the net DMPC. However, when the nanotube−membrane molecule attraction is strong and becomes larger than the membrane molecule−membrane molecule attraction, corresponding to the cases of DN1 and DN2, the effective interaction between the membrane molecules is decreased, leading to an increase of APM as observed in the simulation.

Effect of Embedded Nanotube on the Diffusion Behavior of DMPC. The lateral diffusion is one of the essential processes for biological membranes to function.[50,51] Apart from the influence on membrane structure, it is interesting to know how the embedded tubes interfere with the diffusion behavior of lipid molecules. The lateral mean square displacement (LMSD) was used to study the lateral diffusion behavior of lipids. The lateral diffusion constant was calculated by the Einstein equation:[52]

$$D_T = \lim_{t\to\infty} \frac{1}{2dt}\langle |r(t) - r(0)|^2 \rangle \tag{3}$$

where $r(t)$ is the projection of the center of mass (COM) of the lipid molecule onto the membrane xy plane at time t; d is the number of dimensional degrees of freedom, and $d = 2$ for lateral diffusion.

Figure 3 shows the LMSD plots for DMPC molecules in net DMPC and DN1. The LMSD profiles of DN0, DN2, DN3, and DN4 are very similar to that of DN1. All curves tend to satisfy the Einstein equation in the long run. Linear fits yield the lateral diffusion constants (D_T, Table 3) of 13 × 10^{-8} cm^2/s for net DMPC, which agrees with reported values, both in computational studies (12 × 10^{-8} cm^2/s and 13 × 10^{-8} cm^2/s)[53,54] and experimental studies (12.5 × 10^{-8} cm^2/s and 15.2 × 10^{-8} cm^2/s).[55,56] The same method was used to get the lateral diffusion constants of 4 × 10^{-8} cm^2/s, 4.5 × 10^{-8} cm^2/s, 3.75 × 10^{-8} cm^2/s, 4.5 × 10^{-8} cm^2/s, and 4.75 × 10^{-8} cm^2/s for models DN0, DN1, DN2, DN3, and DN4, respectively. All D_T in models with DWCNT embedded are smaller than that of net DMPC, indicating that DWCNT as an obstacle hinders the diffusion of lipids. However, the lipid molecules exhibit Einstein diffusion behavior in all models.

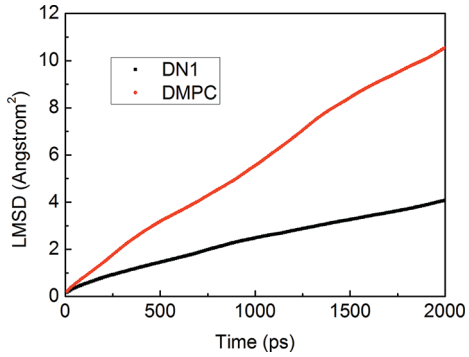

Figure 3. Average lmsd for the COM of the lipids in net DMPC and DN1.

Table 3. Diffusion Constants of DMPC Lipid

	DN0	DN1	DN2	DN3	DN4	net DMPC
D_T (10^{-8} cm^2 s^{-1})	4	4.5	3.75	4.5	4.75	13

The results indicate that the steric interaction with the nanotube reduces the lateral diffusion of the membrane molecule obviously. It should be pointed out that the diffusion behavior of the membrane molecule has not been influenced by the long-range electrostatic interaction, for that embedded with N-DWCNT does not lead to an apparent change of the diffusion constant compared to that embedded with pristine DWCNT.

Effect of Embedded Nanotube on the Diffusion Behavior of Small Polar Molecules Inside Membrane. One of the most important biological functions of a

dx.doi.org/10.1021/jp301864z | J. Phys. Chem. B 2012, 116, 5391−5397

biomembrane is that it is a selectively permeable structure. It might be a source of cellular toxicity if the diffusion behavior of some small polar organic molecules significantly changes with the presence of nanotube in the bilayer.[35] In this study, Urea and ethanol are two general polar molecules used to permeate across biomembrane.

The mean square displacement (msd) was computed to describe the diffusion behavior.

$$D_{\text{eff}} = \lim_{t\to\infty} \frac{1}{2dt}\langle |r(t) - r(0)|^2 \rangle \tag{4}$$

where $r(t)$ is the displacement of the particle at time t, d is the number of dimensional degrees of freedom, and $d = 3$ here.

On the basis of our observations, the diffusion behavior for both urea and ethanol satisfy eq 4. Therefore, we can determine the diffusion constant from the linear fit of Figure 4. The diffusion constants are illustrated in Table 4.

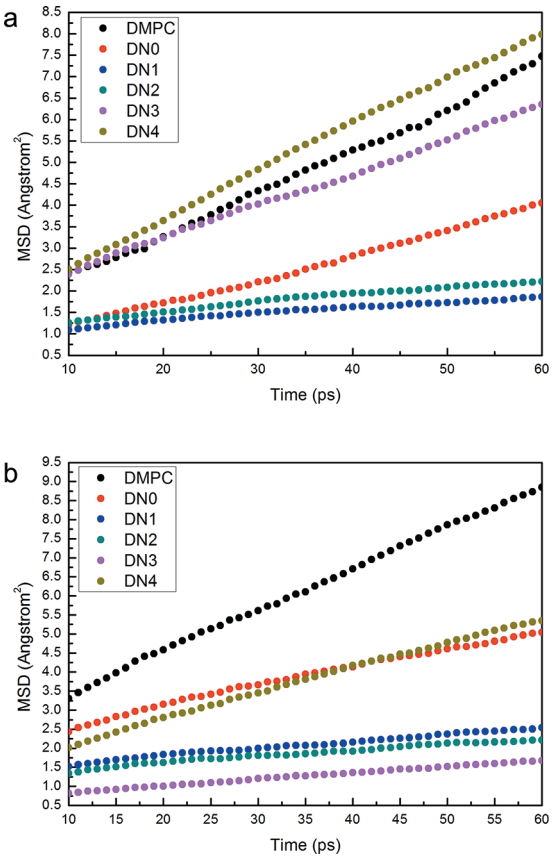

Figure 4. Average msd for the small polar molecules diffusing inside biomembrane. (a) Urea diffuses inside biomembrane. (b) Ethanol diffuses inside biomembrane.

Table 4. Diffusion Constants for Urea and Ethanol Diffuse Inside the DMPC Bilayer

	D of urea (10^{-8} cm^2 s^{-1})	D of ethanol (10^{-8} cm^2 s^{-1})
DN0	95	83
DN1	24	32
DN2	32	27
DN3	128	28
DN4	183	111
net DMPC	167	182

The diffusion constants of urea in models DN0, DN3, and DN4 are in the same order of magnitude with that in net DMPC, while they are one magnitude smaller in models DN1 and DN2 than that in net DMPC, as shown in Table 4. In addition, the diffusion constants of ethanol are in the same order of magnitude in DN0, DN4, and net DMPC, while they are one magnitude smaller in the other three models.

We understand this observation from the concept of an effective interaction theory, within which the effective value of a physical quantity in a real system can be divided into two parts of contributions, namely, the bare value and the interaction-modified value. All the effects of interactions from the environment on the effective value come from the interaction-modified part.

For the present study, we are interested in the diffusion behavior of the polar molecules inside the membrane, which is characterized by the effective diffusion constant D_{eff}. From the Einstein relationship, $D_{\text{eff}} = k_B T/\zeta_{\text{eff}}$, which is a special case of the general fluctuation−dissipation theorem, the behavior of D_{eff}, characteristics of the fluctuation behavior of a system, can be understood by analyzing the effective friction constant ζ_{eff}, characteristics of the response behavior of a system. We define ζ_{eff} as follows

$$\zeta_{\text{eff}} = \zeta_0 + \zeta_1(E) \tag{5}$$

where ζ_0 is the bare friction constant; $\zeta_1(E)$ is the interaction-modified friction constant with all the effects of environment interactions included; E stands for the strength of the interaction. Clearly, the effective friction is dependent on the strength of E. Now we can look into the behavior of the effective diffusion constant.

$$\begin{aligned} D_{\text{eff}} &= \frac{k_B T}{\zeta_{\text{eff}}} \\ &= \frac{k_B T}{\zeta_0 + \zeta_1(E)} \\ &= \frac{k_B T}{\zeta_0\left(1 + \frac{\zeta_1(E)}{\zeta_0}\right)} \\ &\approx \frac{k_B T}{\zeta_0}\left(1 - \frac{\zeta_1(E)}{\zeta_0}\right) \\ &= D_0 - D_1(E) \end{aligned} \tag{6}$$

where we have assumed $\zeta_1(E)/\zeta_1 \ll 1$, namely, the interaction E is weak, and we have defined $D_0 = (k_B T)/\zeta_0$ and $D_1(E) = D_0(\zeta_1(E)/\zeta_0)$.

By this analysis, it is clear that, with the increase of the interaction strength E, $\zeta_1(E)$ increases and $D_1(E)$ in order, leading to a decrease of D_{eff}. This is observed in our simulation, and we illustrate it in Figure 5.

We would like to note that, in our simulations, both the van der Waals interaction and the electrostatic interaction between a small polar molecule and CNT have been computed. It is found that, as for the effects on the diffusion behavior, the electrostatic interaction plays a more important role than the van der Waals interaction, which can be due to the long-range nature of the electrostatic interaction. Therefore, for the interaction-modified friction constant, E, is mainly the strength of the electrostatic interaction.

dx.doi.org/10.1021/jp301864z | J. Phys. Chem. B 2012, 116, 5391−5397

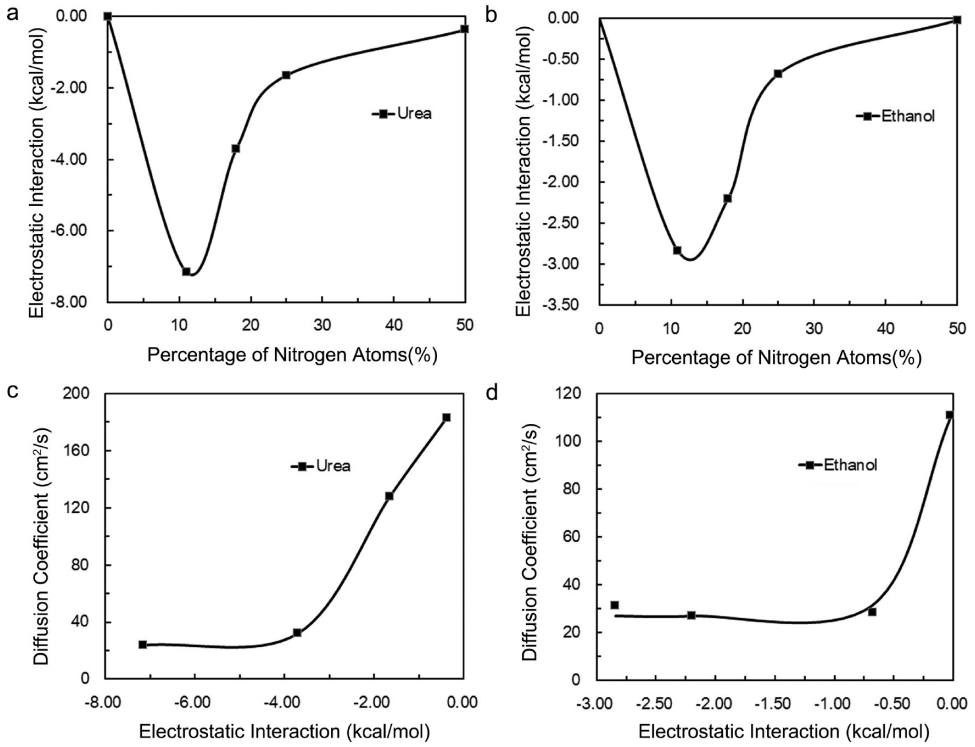

Figure 5. Correlation of electrostatic interaction between N-DWCNT and penetrants with diffusion constant of small polar molecules. (a) Electrostatic interaction energy between N-DWCNT and urea. (b) Electrostatic interaction energy between N-DWCNT and ethanol. (c) The relationship of diffusion behavior for urea inside the membrane and electrostatic interaction energy between N-DWCNT and urea. (d) The relationship of diffusion behavior for ethanol inside the membrane and electrostatic interaction energy between N-DWCNT and ethanol.

CONCLUSIONS

We found that the embedded CNT reduces the entropy of interfacial lipid molecules because of its rigid and unaccommodating structure and leads to fewer conformational states available to DMPC molecules adjacent to the tube, while the long-range electrostatic interaction with the N-DWCNT excites the conformational fluctuation of lipid molecules. The curvature of embedded nanotube could also influence the flexibility of lipid molecules.

The packing density of DMPC membrane in models DN0, DN3, and DN4 are almost not disturbed by the embedded DWCNT compared to that of net DMPC, while the organization of membrane is relaxed in models DN1 and DN2. This phenomenon can be understood from the viewpoint of the effective interaction. When the interaction between the tube and the membrane molecule is weak, such as in the cases of DN0, DN3, and DN4, the organization of the membrane molecule is almost unaffected. However, when the attraction between the tube and the membrane molecule strongly increases, such as in the cases of DN1 and DN2, the attraction among the membrane molecules decreases effectively, leading to an increase of the APM.

All lateral diffusion constant D_T of lipid molecules in models with embedded DWCNT are smaller than that of net DMPC, indicating that DWCNT as an obstacle hinders the diffusion of lipids. The steric interaction with the nanotube reduces the lateral diffusion of the membrane molecule. The long-range electrostatic interaction is not strong enough to influence the lateral diffusion behavior of the membrane molecule.

As for the diffusion behavior of small polar molecules inside the membrane in the presence of the nanotube, we find that, with the increase of the strength of electrostatic interaction E, interaction-modified friction $\zeta_1(E)$ increases, which leads to the decrease of diffusion constant D_{eff}.

AUTHOR INFORMATION

Corresponding Author

*(X.L.) Tel: +86-10-8825-6856. Fax: +86-10-8825-6701. E-mail: lixy@gucas.ac.cn. (Y.Z.) Tel: +86-10-8823-6456. Fax: +86-10-8823-3191. E-mail: zhaoyl@nanoctr.cn.

Notes

The authors declare no competing financial interest.

ACKNOWLEDGMENTS

This work was supported by the National Natural Science Foundation of China (projects 21144001 and 21104094), 973 program (2011CB933400 and 2010CB934004), the Knowledge Innovation Program of Chinese Academy of Sciences, and the President Fund of GUCAS. This work is supported by the Supercomputing Center of Chinese Academy of Sciences.

REFERENCES

(1) Houili, H.; Tutis, E.; Izquierdo, R. *Org. Electron.* **2010**, *11*, 514−520.

(2) Gunasekera, U. A.; Pankhurst, Q. A.; Douek, M. *Targeted Oncol.* **2009**, *4*, 169−181.

(3) McBain, S. C.; Yiu, H. H. P.; Dobson, J. *Int. J. Nanomed.* **2008**, *3*, 169−180.

(4) Gu, F. X.; Karnik, R.; Wang, A. Z.; Alexis, F.; Levy-Nissenbaum, E.; Hong, S.; Langer, R. S.; Farokhzad, O. C. *Nano Today* **2007**, *2*, 14−21.

(5) Alivisatos, A. P.; Gu, W. W.; Larabell, C. Quantum Dots As Cellular Probes. *Annu. Rev. Biomed. Eng.* **2005**, *7*, 55−76.

(6) Feris, K.; Otto, C.; Tinker, J.; Wingett, D.; Punnoose, A.; Thurber, A.; Kongara, M.; Sabetian, M.; Quinn, B.; Hanna, C.; Pink, D. *Langmuir* **2010**, *26*, 4429−4436.
(7) Deng, X.; Luan, Q.; Chen, W.; Wang, Y.; Wu, M.; Zhang, H.; Jiao, Z. *Nanotechnology* **2009**, *20*, 115101.
(8) Hanley, C.; Layne, J.; Punnoose, A.; Reddy, K. M.; Coombs, I.; Coombs, A.; Feris, K.; Wingett, D. *Nanotechnology* **2008**, *19*, 295103.
(9) Reddy, K. M.; Feris, K.; Bell, J.; Wingett, D. G.; Hanley, C.; Punnoose, A. *Appl. Phys. Lett.* **2007**, *90*, 213902.
(10) Brunner, T. J.; Wick, P.; Manser, P.; Spohn, P.; Grass, R. N.; Limbach, L. K.; Bruinink, A.; Stark, W. J. *Environ. Sci. Technol.* **2006**, *40*, 4374−4381.
(11) Theron, J.; Walker, J. A.; Cloete, T. E. *Crit. Rev. Microbiol.* **2008**, *34*, 43−69.
(12) Barth, J. V.; Costantini, G.; Kern, K. *Nature* **2005**, *437*, 671−679.
(13) Fischer, H. C.; Chan, W. C. W. *Curr. Opin. Biotechnol.* **2007**, *18*, 565−571.
(14) Makarucha, A. J.; Todorova, N.; Yarovsky, I. *Eur. Biophys. J.* **2011**, *40*, 103−115.
(15) Yang, K.; Ma, Y.-Q. *Nat. Nanotechnol.* **2010**, *5*, 579−583.
(16) Monticelli, L.; Salonen, E.; Ke, P. C.; Vattulainen, I. *Soft Matter* **2009**, *5*, 4433−4445.
(17) Ghorai, P. K.; Glotzer, S. C. *J. Phys. Chem. C* **2007**, *111*, 15857−15862.
(18) Sachs, J. N.; Woolf, T. B. *J. Am. Chem. Soc.* **2003**, *125*, 8742−8743.
(19) Bedrov, D.; Smith, G. D.; Davande, H.; Li, L. *J. Phys. Chem. B* **2008**, *112*, 2078−2084.
(20) Smith, G. D.; Bedrov, D. *Biophys. J.* **2007**, 65A−66A.
(21) Wong-Ekkabut, J.; Baoukina, S.; Triampo, W.; Tang, I. M.; Tieleman, D. P.; Monticelli, L. *Nat. Nanotechnol.* **2008**, *3*, 363−368.
(22) Li, L.; Davande, H.; Bedrov, D.; Smith, G. D. *J. Phys. Chem. B* **2007**, *111*, 4067−4072.
(23) D'Rozario, R. S. G.; Wee, C. L.; Wallace, E. J.; Sansom, M. S. P. *Nanotechnology* **2009**, *20*, 115102.
(24) Qiao, R.; Roberts, A. P.; Mount, A. S.; Klaine, S. J.; Ke, P. C. *Nano Lett.* **2007**, *7*, 614−619.
(25) Ginzburg, V. V.; Balijepailli, S. *Nano Lett.* **2007**, *7*, 3716−3722.
(26) Mailaender, V.; Landfester, K. *Biomacromolecules* **2009**, *10*, 2379−2400.
(27) Titov, A. V.; Kral, P.; Pearson, R. *ACS Nano* **2010**, *4*, 229−234.
(28) Shi, X.; Kong, Y.; Gao, H. *Acta Mech. Sin.* **2008**, *24*, 161−169.
(29) Wallace, E. J.; Sansom, M. S. P. *Nano Lett.* **2008**, *8*, 2751−2756.
(30) Wallace, E. J.; Sansom, M. S. P. *Nanotechnology* **2009**, *20*, 045101.
(31) Li, Y.; Gu, N. *J. Phys. Chem. B* **2010**, *114*, 2749−2754.
(32) Li, Y.; Chen, X.; Gu, N. *J. Phys. Chem. B* **2008**, *112*, 16647−16653.
(33) Verma, A.; Stellacci, F. *Small* **2010**, *6*, 12−21.
(34) Nielsen, S. O.; Ensing, B.; Ortiz, V.; Moore, P. B.; Klein, M. L. *Biophys. J.* **2005**, *88*, 3822−3828.
(35) Liu, J.; Hopfinger, A. J. *Chem. Res. Toxicol.* **2008**, *21*, 459−466.
(36) Liu, B.; Li, X.; Li, B.; Xu, B.; Zhao, Y. *Nano Lett.* **2009**, *9*, 1386−1394.
(37) Yang, Y.; Li, X.; Jiang, J.; Du, H.; Zhao, L.; Zhao, Y. *ACS Nano* **2010**, *4*, 5755−5762.
(38) Jia, G.; Wang, H. F.; Yan, L.; Wang, X.; Pei, R. J.; Yan, T.; Zhao, Y. L.; Guo, X. B. *Environ. Sci. Technol.* **2005**, *39*, 1378−1383.
(39) Elias, A. L.; Carrero-Sanchez, J. C.; Terrones, H.; Endo, M.; Laclette, J. P.; Terrones, M. *Small* **2007**, *3*, 1723−1729.
(40) de Groot, B. L.; Grubmuller, H. *Science* **2001**, *294*, 2353−2357.
(41) Murata, K.; Mitsuoka, K.; Hirai, T.; Walz, T.; Agre, P.; Heymann, J. B.; Engel, A.; Fujiyoshi, Y. *Nature* **2000**, *407*, 599−605.
(42) Phillips, J. C.; Braun, R.; Wang, W.; Gumbart, J.; Tajkhorshid, E.; Villa, E.; Chipot, C.; Skeel, R. D.; Kale, L.; Schulten, K. *J. Comput. Chem.* **2005**, *26*, 1781−1802.
(43) Vanommeslaeghe, K.; Hatcher, E.; Acharya, C.; Kundu, S.; Zhong, S.; Shim, J.; Darian, E.; Guvench, O.; Lopes, P.; Vorobyov, I.; MacKerell, A. D., Jr. *J. Comput. Chem.* **2010**, *31*, 671−690.
(44) Feller, S. E.; MacKerell, A. D. *J. Phys. Chem. B* **2000**, *104*, 7510−7515.
(45) Essmann, U.; Perera, L.; Berkowitz, M. L.; Darden, T.; Lee, H.; Pedersen, L. G. *J. Chem. Phys.* **1995**, *103*, 8577−8593.
(46) Klauda, J. B.; Brooks, B. R.; Pastor, R. W. *J. Chem. Phys.* **2006**, *125*, 144710.
(47) Singer, S. J.; Nicolson, G. L. *Science* **1972**, *175*, 720−&.
(48) Humphrey, W.; Dalke, A.; Schulten, K. *J. Mol. Graphics Model.* **1996**, *14*, 33−38.
(49) Bernal, J. D. *Nature* **1959**, *183*, 141−147.
(50) Helmreich, E. J. M. *Biophys. Chem.* **2003**, *100*, 519−534.
(51) Singer, S. J.; Nicolson, G. L. *Science* **1972**, *175*, 720−731.
(52) Einstein, A. *Ann. Phys.* **1905**, *17*, 549−560.
(53) Patra, M.; Karttunen, M.; Hyvonen, M. T.; Falck, E.; Vattulainen, I. *J. Phys. Chem. B* **2004**, *108*, 4485−4494.
(54) Lindahl, E.; Edholm, O. *J. Chem. Phys.* **2001**, *115*, 4938−4950.
(55) Scheidt, H. A.; Huster, D.; Gawrisch, K. *Biophys. J.* **2005**, *89*, 2504−2512.
(56) Vaz, W. L. C.; Clegg, R. M.; Hallmann, D. *Biochemistry* **1985**, *24*, 781−786.